Particle-vibration coupling in proton decay of near-spherical nuclei

Cary N. Davids and Henning Esbensen
Physics Division, Argonne National Laboratory, Argonne, Illinois 60439

(Received 10 May 2001; published 22 August 2001)

A particle-vibration coupling model is applied to explain the spectroscopic factors and decay rates of odd-A and odd-odd near-spherical proton emitters, as well as the branching ratio for the recently observed fine structure in the decay of ^{145}Tm. In addition, a deformed solution for ^{145}Tm with $K=5/2^-$ is presented. Using particle-vibration coupling, good agreement is achieved with observed spectroscopic factors for the near-spherical emitters, including $d_{3/2}$ cases. For the odd-odd emitters, the unpaired neutron is treated as a spectator. The single-particle potential used in this work has the same parameters as that used to successfully describe the decay rates of the deformed proton emitters ^{131}Eu and ^{141}Ho.

DOI: 10.1103/PhysRevC.64.034317 PACS number(s): 23.50.+z, 21.10.Tg, 24.10.Eq

I. INTRODUCTION

The observation of proton radioactivity has provided nuclear structure information on nuclides lying beyond the proton drip line. In the past, the proton emitters in the region $68<Z<82$ have been treated as spherical. Their decay rates were calculated using a one-dimensional semiclassical WKB barrier approximation, yielding information on the angular momentum carried off by the proton [1]. Subsequent work has provided a full quantum mechanical description of the decay rates for spherical emitters [2–4].

As more data became available, the spectroscopic factors for the spherical proton emitters, defined as the ratio of observed and calculated decay rates

$$S_{exp}^{lj}=\frac{\Gamma_{exp}^{lj}}{\Gamma_{calc}^{lj}}$$

were observed to decrease with increasing Z of the daughter. The part of the spectroscopic factor arising from residual pairing interactions produces a component in the daughter state wave function representing pairs of particles already occupying the same orbital as the decaying proton. When this is taken into account, good agreement with the observed spectroscopic factors is obtained for $h_{11/2}$ and $s_{1/2}$ emitters, while the observed spectroscopic factors for $d_{3/2}$ states are consistently lower than predicted by a low-seniority shell model calculation [5] or BCS calculations [3].

The recent observation of fine structure in the proton decay of ^{145}Tm [6] suggests that the simple spherical approach does not provide a full description of the proton emission process for spherical or near-spherical nuclides. In this picture, the conservation of angular momentum only allows decay to the ground state, with no possibility of calculating decay to excited states of the daughter. In the case of ^{145}Tm, two proton groups were observed with the same half-life of 3.0(3) μs, one populating the ground state and the other populating the first 2^+ state of the daughter nucleus ^{144}Er at 0.326 MeV with a branching ratio of 12(3)%.

At first glance this suggests a deformed emitter, and we have used the formalism of Ref. [7] to calculate, in the adiabatic limit, the half-lives and 2^+ branching ratios for ^{145}Tm with ground-state spins $\frac{1}{2}^{\pm}\leqslant J\leqslant\frac{11}{2}^{\pm}$. These are shown in Table I, using prolate and oblate quadrupole deformations of $|\beta_2|=0.18$, as suggested by the excitation energy in ^{144}Er of 0.326 MeV. To relate the calculated and experimental decay rates, a spectroscopic factor near 0.5 must be used. This reflects the fact that in a deformed nucleus where the decaying Nilsson level is close to the Fermi surface, the probability that this particular level is unoccupied in the daughter nucleus is about 0.5. The branching ratios can be compared directly, since the spectroscopic factors cancel. We see that the oblate deformed solution with $K=\frac{5}{2}^-$ comes quite close to agreeing with the experimental half-life and branching ratio values of 3.0(3) μs and 12(3)% [6], with a spectroscopic factor of 0.74(9). However, this state is not expected to be at the Fermi level for $^{145}_{69}$Tm; Ferreira and Maglione [8] show that the oblate $K=5/2^-$ state is at the Fermi level for $^{151}_{71}$Lu. Although recent calculations [9–11] predict prolate rather than oblate deformation for the ground states of ^{145}Tm

TABLE I. Calculation of the proton half-life $T_{1/2}$ and 2^+ branching ratio (BR) for ^{145}Tm using the deformed formalism of Ref. [7]. A spectroscopic factor of 1 has been assumed (see text). Results are given for prolate and oblate quadrupole deformations of magnitude $|\beta_2|=0.18$. The experimental values are $T_{1/2}=3.0(3)$ μs and BR=12(3)% [6].

	$\beta=+0.18$		$\beta=-0.18$	
J^π	$T_{1/2}$	BR (%)	$T_{1/2}$	BR (%)
$\frac{1}{2}^-$	1.7 ns	1.9	0.2 μs	9.6
$\frac{3}{2}^-$	3.0 ns	0.6	29 ns	0.6
$\frac{5}{2}^-$	0.3 μs	3.0	2.2 μs	21
$\frac{7}{2}^-$	0.5 μs	1.0	0.16 μs	1.0
$\frac{9}{2}^-$	0.2 ms	32	0.1 ms	24
$\frac{11}{2}^-$	5.9 μs	1.0	2.5 μs	1.1
$\frac{1}{2}^+$	0.6 ns	0.2	0.2 ns	0.1
$\frac{3}{2}^+$	47 ns	22	2.7 ns	0.8
$\frac{5}{2}^+$	2.6 ns	0.8	9.3 ns	0.8
$\frac{7}{2}^+$	0.67 μs	0.9	0.37 μs	0.9
$\frac{9}{2}^+$	6.0 μs	1.0	1.6 μs	1.1
$\frac{11}{2}^+$	6.8 ms	34	2.7 ms	24

and its decay daughter ^{144}Er, our decay rate results are not compatible with the prolate possibility.

Besides the oblate-deformed $J=5/2^-$ solution, we now consider another alternative: ^{145}Tm and other near-spherical proton emitters may have a time-averaged spherical shape, but their wave functions contain other components due to particle-vibration coupling. A look at the low-lying energy levels of the even-even daughters of the odd-A proton emitters between $^{145}_{69}$Tm and $^{177}_{81}$Tl suggests that this assumption may be valid. In most cases the ratio of excitation energies $E_x(4^+)/E_x(2^+)$ lie in the range 2.0–2.4, characteristic of an anharmonic vibrator. This indicates that the interaction between the last proton and the core nucleus should include particle-vibration coupling to the first 2^+ state of the daughter nucleus. Possible exceptions are discussed in Sec. III.

The case of an odd-A, $J=11/2^-$ proton emitter will serve as an example. In addition to the $j=11/2^-\otimes 0^+$ component, which can only decay to the daughter ground state, the parent wave function will contain five additional components arising from $j=7/2^-\otimes 2^+$ through $j=15/2^-\otimes 2^+$, all coupled to $J=11/2^-$. These latter components can only decay to the 2^+ state of the daughter, with the decay widths dependent on the amount of energy available, the size of these components, and the l values involved. The consequent reduction in the ground-state proton decay spectroscopic factor due to such coupling has already been considered by Semmes for ^{151}Lu$(3/2^+)$ [12].

In Sec. II we discuss the calculation of proton decay rates using the coupled-channels formalism with a quadrupole particle-vibration coupling. In Sec. III we present applications of the method to several proton emitters.

II. COUPLED-CHANNELS APPROACH WITH PARTICLE-VIBRATION COUPLING

In order to calculate the proton decay rate, we need to determine the wave function of a nucleus consisting of a single proton interacting with an even-even core. We consider only the 0^+ ground state and the first excited 2^+ state of the core, and, as in [7], search for narrow unbound resonances in this coupled system. Here, however, the average core shape is spherical, with vibrational coupling to the proton. As in [7], we expand the total wave function for a given total spin (I,M) of the system as

$$\Psi_{IM}(\mathbf{r})=\sum_{lj\lambda}\frac{\phi^{I}_{lj\lambda}(r)}{r}|l(j\lambda)IM\rangle, \tag{1}$$

where

$$|l(j\lambda)IM\rangle=\sum_{m\mu}\langle jm\lambda\mu|IM\rangle|\lambda\mu\rangle|ljm\rangle \tag{2}$$

is the channel-spin wave function, obtained by coupling the single-particle spin-angular wave functions $|ljm\rangle$ to the core wave function $|\lambda\mu\rangle$. When $\lambda=0$, $l=l_o$, and $j=I$.

The single-particle potential for a proton interacting with a spherical nucleus includes the nuclear and spin-orbit interactions and the Coulomb potential,

$$V_{\rm sp}(r)=V_N(r)+V_{ls}(r)\mathbf{l}\cdot\mathbf{s}+V_C(r). \tag{3}$$

Our parametrization is given in Appendix A of Ref. [7]. There we discussed the generalization to the case of a deformed core nucleus. Here we consider a vibrational core nucleus and employ the total Hamiltonian

$$H=-\frac{\hbar^2}{2m_0}\Delta+V_{\rm sp}+H_{\rm vib}+\delta V_{\rm vib}, \tag{4}$$

where m_0 is the reduced mass and $H_{\rm vib}$ is the intrinsic vibrational Hamiltonian of the daughter nucleus, with eigenvalues E_0 for the 0^+ ground state and E_2 for the first excited 2^+ state. The last term is the coupling between the single-particle motion and the vibrational excitation, which we now derive.

The nuclear one-body interaction $V_N(r)$, and also the charge density $\rho_D(r)$ of the daughter nucleus, are parametrized in terms of the Fermi function $f([r-R]/a)=[1+\exp\{(r-R)/a\}]^{-1}$, cf. Ref. [7]. On average the core nucleus has a spherical shape, but it is susceptible to quadrupole vibrations. Thus the nuclear surface is expressed as $R=R_0[1+\Sigma_\mu\alpha_{2\mu}Y^*_{2\mu}(\hat{r})]$, where $\alpha_{2\mu}$ are the vibrational amplitudes. With this parametrization, we expand the Fermi function to first order in the vibrational amplitudes,

$$f\left(\frac{r-R}{a}\right)\approx f\left(\frac{r-R_0}{a}\right)-R_0\sum_\mu\alpha_{2\mu}Y^*_{2\mu}(\hat{r})\frac{d}{dr}f\left(\frac{r-R_0}{a}\right). \tag{5}$$

We can now include the effect of the first-order vibrational term in Eq. (5) in the nuclear interaction, and also the Coulomb interaction derived from the charge density as in Eq. (A5) of Ref. [7]. Thus we obtain the vibrational coupling

$$\delta V_{\rm vib}(r,\alpha_{2\mu})=F_{\rm vib}(r)\sum_\mu\alpha_{2\mu}Y^*_{2\mu}(\hat{r}), \tag{6a}$$

$$F_{\rm vib}(r)=-R_N\frac{dV_N(r)}{dr}-R_C\frac{4\pi Z_De^2}{5}\int dr'r'^2\frac{d\rho_D(r')}{dr'}\frac{r^2_<}{r^3_>}, \tag{6b}$$

where R_N and R_C are the radii associated with the nuclear interaction and the charge density of the core nucleus, respectively, and $r_<=\min(r,r')$, and $r_>=\max(r,r')$.

Using the total Hamiltonian (4), we can now project the Schrödinger equation $H\Psi_{IM}=E\Psi_{IM}$ with the channel-spin wave function $|l(j\lambda)IM\rangle$. Inserting the expression (1) we thus obtain the following set of coupled radial equations:

$$\left[\frac{\hbar^2}{2m_0}\left(-\frac{d^2}{dr^2}+\frac{l(l+1)}{r^2}\right)+V_{\rm sp}(r)+E_\lambda-E\right]\phi^I_{lj\lambda}(r)$$
$$=\sum_{l'j'\lambda'}\left\langle l(j\lambda)IM\left|\sum_\mu\alpha_{2\mu}Y^*_{2\mu}(\hat{r})\right|l'(j'\lambda')IM\right\rangle$$
$$\times F_{\rm vib}(r)\phi^I_{l'j'\lambda'}(r), \tag{7}$$

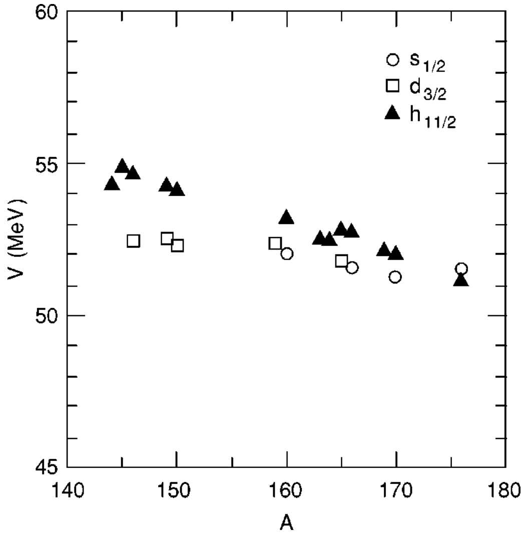

FIG. 1. Depths of the nuclear potential $V_N(r)$ for the proton emitters considered in this work, plotted as a function of daughter nucleus mass A.

where λ and λ' can have the values of either 0 or 2, and the off-diagonal character of the vibrational coupling restricts the sum to $\lambda' \neq \lambda$. We first choose a particular single-particle orbit (l_0, I) associated with the decay to the $\lambda = 0^+$ ground state of the daughter nucleus. The additional single-particle orbits (l,j) to be considered in the coupled equations include $j = |I-2|, \ldots, I+2$, associated with the $\lambda = 2^+$ excited state. Moreover, the orbital angular momenta l are restricted by parity conservation, since $l + 2 - l_0$ must be even.

The matrix element on the right-hand side of Eq. (7) is Hermitian. It can therefore be calculated, without loss of generality, for $\lambda = 2$ and $\lambda' = 0$,

$$\left\langle l(j2)IM \left| \sum_{\mu} \alpha_{2\mu} Y^*_{2\mu}(\hat{r}) \right| l'(I0)IM \right\rangle = \sum_{m\mu} \langle jm2\mu | IM \rangle \alpha_2^{(0)} \langle ljm | Y^*_{2\mu}(\hat{r}) | l'IM \rangle = \sqrt{\frac{5}{4\pi}} \alpha_2^{(0)} \langle I \tfrac{1}{2} 20 | j \tfrac{1}{2} \rangle, \tag{8}$$

where $\alpha_2^{(0)} = \langle 2\mu | \alpha_{2\mu} | 00 \rangle$ is the vibrational transition matrix element.

In order to solve the coupled equations, a value of $\alpha_2^{(0)}$ must be determined. Using Eqs. (6-52) and (6-65) of [13], we find

$$\alpha_2^{(0)} = \frac{\beta_2}{\sqrt{5}}, \tag{9}$$

where β_2 is the total zero-point amplitude. It can be related to the $B(E2\uparrow)$ for the electromagnetic transition between the ground state and the first excited 2^+ state of the core:

$$B(E2\uparrow) = \left(\frac{3}{4\pi} Z_D e R_o^2 \right)^2 \beta_2^2, \tag{10}$$

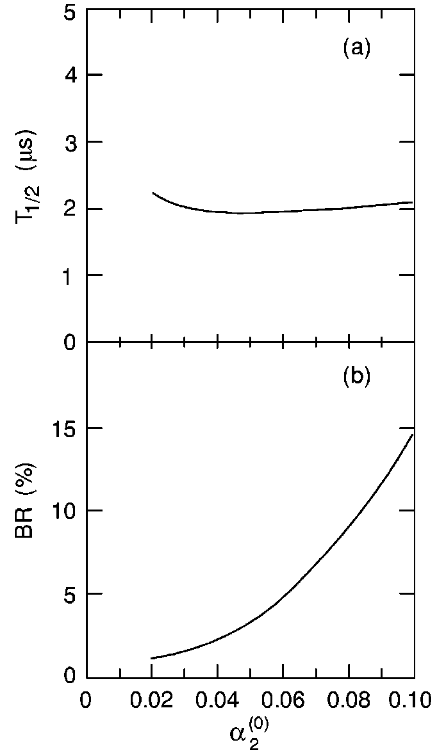

FIG. 2. (a) Calculated proton decay half-life for ^{145}Tm as a function of $\alpha_2^{(0)}$, for an initial spin $J = 11/2^-$. A 2^+ excitation energy of 0.326 MeV in the daughter nucleus has been used. (b) Calculated branching ratio $\Gamma(2^+)/[\Gamma(0^+) + \Gamma(2^+)]$ for ^{145}Tm, in percent. The spectroscopic factors for both branches have been set to unity for this figure (see Sec. III A).

where Z_D is the atomic number of the daughter nucleus. An empirical relation for $B(E2\uparrow)$ [14] enables us to estimate to better than 25% the size of the amplitude $\alpha_2^{(0)}$ as

$$\alpha_2^{(0)} = \frac{218}{A\sqrt{E_x(2^+)}}, \tag{11}$$

where A is the core mass number and $E_x(2^+)$ is in keV.

As in Ref. [7], the solutions of the coupled equations are matched to Coulomb waves at a relatively small distance, $r_m = 16$ fm, outside the range of the nuclear force. We

TABLE II. Calculated intensities $C^2_{lj\lambda}$ $(\Sigma_{lj\lambda} C^2_{lj\lambda} = 1)$ and decay widths Γ_{J_f} for the six components of the ^{145}Tm ground-state wave function. All configurations are coupled to spin $J_i = \frac{11}{2}^-$.

Configuration	$C^2_{lj\lambda}$	$\Gamma_{0^+}(10^{-16}$ MeV)	$\Gamma_{2^+}(10^{-16}$ MeV)
$11/2^- \otimes 0^+$	0.33	2.04	[a]
$7/2^- \otimes 2^+$	0.04	[a]	0.23
$9/2^- \otimes 2^+$	$\leqslant 0.01$	[a]	$\leqslant 0.01$
$11/2^- \otimes 2^+$	0.62	[a]	0.01
$13/2^- \otimes 2^+$	$\leqslant 0.01$	[a]	$\leqslant 0.01$
$15/2^- \otimes 2^+$	0.01	[a]	$\leqslant 0.01$

[a]Decay not allowed.

TABLE III. Results of particle-vibrational coupling calculations for odd-A spherical proton emitters with spin J_i. Experimental uncertainties in the proton energies and half-lives have been included in the uncertainties for the experimental spectroscopic factors S_{exp}. The calculated spectroscopic factors S_{th} are taken from Ref. [5].

Nuclide	J_i	$E_x(2^+)$ (keV)	$\alpha_2^{(0)}$	Γ(calc) (10^{-16} MeV)	Γ(exp) (10^{-16} MeV)	S_{exp}	S_{th}
^{145}Tm	$\frac{11}{2}^-$	326 [6]	0.084	$2.03(J_f=0^+)$	1.34 [6]	0.66(8)	0.78
^{145}Tm	$\frac{11}{2}^-$	326 [6]	0.084	$0.22(J_f=2^+)$	0.18 [6]	0.82(24)	0.99[a]
^{147}Tm^m	$\frac{3}{2}^+$	510 [b]	0.066	1.58×10^{-2}	1.27×10^{-2} [18]	0.80(13)	0.78
^{147}Tm	$\frac{11}{2}^-$	510 [b]	0.066	1.20×10^{-6}	1.18×10^{-6} [18]	0.98(36)	0.78
^{151}Lu^m	$\frac{3}{2}^+$	600 [b]	0.059	0.625	0.285 [19]	0.46(12)	0.67
^{151}Lu	$\frac{11}{2}^-$	600 [b]	0.059	4.98×10^{-5}	3.65×10^{-5} [19]	0.73(21)	0.67
^{161}Re	$\frac{1}{2}^+$	610 [20]	0.055	2.20×10^{-2}	1.23×10^{-2} [21]	0.56(12)	0.44
^{161}Re^m	$\frac{11}{2}^-$	610 [20]	0.055	3.45×10^{-5}	1.37×10^{-5} [21]	0.40(9)	0.44
^{165}Ir$^{(m)}$	$\frac{11}{2}^-$	548 [22]	0.057	3.07×10^{-2}	1.31×10^{-2} [5]	0.43(10)	0.33
^{167}Ir	$\frac{1}{2}^+$	431 [22]	0.063	1.07×10^{-4}	4.15×10^{-5} [5]	0.39(11)	0.33
^{167}Ir^m	$\frac{11}{2}^-$	431 [22]	0.063	1.65×10^{-6}	6.08×10^{-7} [5]	0.37(12)	0.33
^{171}Au	$\frac{1}{2}^+$	509 [23]	0.057	0.704	0.268 [24]	0.38(23)	0.22
^{171}Au^m	$\frac{11}{2}^-$	509 [23]	0.057	9.33×10^{-3}	2.06×10^{-3} [5]	0.22(4)	0.22
^{177}Tl	$\frac{1}{2}^+$	613 [25]	0.050	1.20×10^{-4}	6.84×10^{-5} [24]	$0.57(^{+58}_{-41})$	0.11
^{177}Tl^m	$\frac{11}{2}^-$	613 [25]	0.050	0.232	1.01×10^{-2} [24]	0.044(12)	0.11

[a]See text.
[b]Estimated from energy systematics.

search for the proton resonance by varying the depth of the nuclear potential, and use the boundary conditions

$$\phi^I_{lj\lambda}(r)=N^I_{lj\lambda}G_l(k_\lambda r) \quad \text{at} \quad r=r_m. \tag{12}$$

Here $\hbar k_\lambda=\sqrt{2m_0(E-E_\lambda)}$ is the momentum of the emitted proton, and $G_l(k_\lambda r)$ is the irregular Coulomb function. The wave functions are normalized as in [7]. The partial decay widths are then obtained from

$$\Gamma_{I\lambda}=\sum_{lj}\Gamma^I_{lj\lambda},$$

where

$$\Gamma^I_{lj\lambda}=\frac{\hbar^2 k_\lambda}{m_0}|N^I_{lj\lambda}|^2. \tag{13}$$

We refer to this as the direct method [4] because the decay rate is determined directly from the matching amplitudes (12).

As in Ref. [7], we also use the distorted wave Green's function method to estimate the influence of the long-ranged Coulomb quadrupole interaction on the decay rate. The distorted wave amplitudes, to be inserted in Eq. (13), are

$$N^{\rm DW}_{lj\lambda}=-\frac{2m_0}{\hbar^2 k_\lambda}\int_0^{r_{int}}dr\,rF_l(k_\lambda r)\left\langle l(j\lambda)IM\middle| V_{\rm sp}+\delta V_{\rm vib} - \frac{Z_De^2}{r}\middle|\Psi_{IM}(\mathbf{r})\right\rangle, \tag{14}$$

where $F_l(k_\lambda r)$ is the regular Coulomb wave function. The integration over r is taken out to $r_{int}=100$ fm, after first extrapolating the radial wave functions of the resonance solution Ψ_{IM} beyond r_m, according to Eq. (12). The corrections introduced here amount to a few percent, compared to the direct method. We remind the reader that the two methods give identical results when we choose $r_{int}=r_m$, cf. Refs. [7,15].

III. APPLICATIONS TO NEAR-SPHERICAL PROTON EMITTERS

We have used the coupled-channels Green's function method described above to calculate the proton decay rates of both odd-A and odd-odd spherical proton emitters whose even-even core nuclei display vibrational properties. Since we are dealing with nuclei having $68<Z<82$, the $1h_{11/2}$, $2d_{3/2}$, $3s_{1/2}$, and higher shell model orbitals are available for inclusion in the coupled equations. Where known, experimental values for the excitation energy of the first 2^+ state in the core have been used in Eq. (11). In other cases systematic estimates for the excitation energies have been used.

The potential parameters used are identical to those used to successfully describe the decay of the deformed proton emitters ^{131}Eu and ^{141}Ho [7]. We use the radius parameter $R_N=1.25A^{1/3}$ fm and diffuseness $a_N=0.65$ fm for the nuclear and spin-orbit interactions, and for the Coulomb potential we use $R_C=1.22A^{1/3}$ fm and diffuseness $a_C=0.56$ fm. As in Ref. [7], we set the spin-orbit depth $V_{so}=10$ MeV fm^2. The depth of the nuclear potential is varied for each case to achieve a resonant solution. It lies between 51 and 55 MeV for all cases as is shown in Fig. 1. The

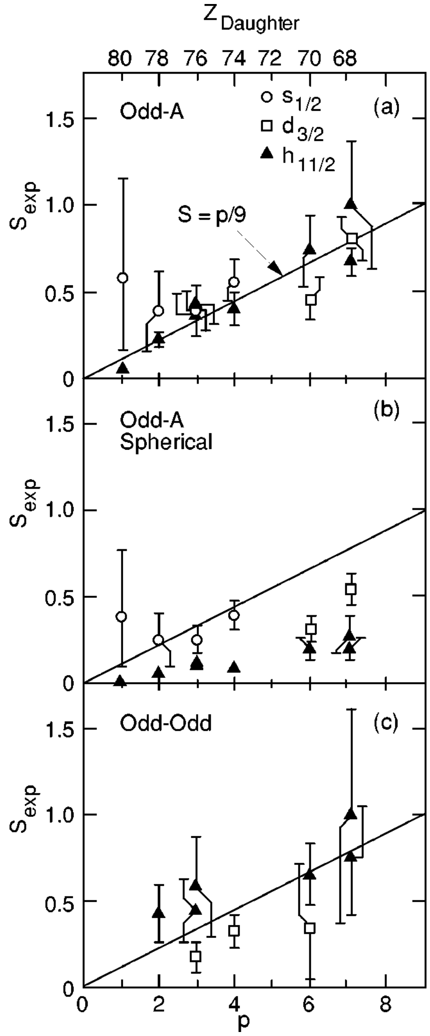

FIG. 3. (a) Experimental spectroscopic factors S_{exp} calculated with particle-vibration coupling for the odd-A proton emitters, plotted as a function of p, the number of pairs of proton holes below $Z=82$ possessed by the daughter nucleus. The atomic number of the daughter nucleus Z_D is also shown, with $Z_D=82-2p$. (b) Experimental spectroscopic factors for spherical odd-A proton emitters (particle-vibration coupling set to zero). (c) Same as (a) except for odd-odd proton emitters.

smooth A dependence of the well depths for different orbitals in Fig. 1 is confirmation of the single-particle character of the resonances.

For odd-A proton emitters the decay widths to the ground and first 2^+ state of the core have each been calculated, and thus both absolute rates and branching ratios can be compared with experimental data. We have not included calculations for ^{155}Ta and ^{157}Ta, whose daughter nuclei ^{154}Hf and ^{156}Hf do not appear to be vibrational. The low-lying structure of these even-even nuclei has been interpreted as $\pi(h_{11/2})^{-4}$ [16] and $\nu(f_{7/2})^2$ [17], respectively, rather than being collective in nature.

For the odd-odd emitters, only the decay width to the daughter ground state is presented here. The unpaired neutron is considered to be a spectator in these calculations, and the assumed core nucleus is the even-even nucleus $(Z-1, A-2)$. Again, we have not included calculations for ^{156}Ta, whose core nucleus ^{154}Hf does not appear to be vibrational.

A. Proton decay of ^{145}Tm

As mentioned in Sec. I, fine structure has been observed in the decay of ^{145}Tm, with a ground state half-life of 3.0(3) μs and a 2^+ branching ratio of 12(3)% [6]. Using the experimental ^{144}Er 2^+ excitation energy of 0.326 MeV in Eq. (11) leads to an amplitude $\alpha_2^{(0)}$ of 0.084. Figure 2 shows the resulting half-life and 2^+ branching ratio calculated as a function of $\alpha_2^{(0)}$ for an initial spin $J=11/2^-$. It is seen that the half-life is quite insensitive to this parameter, while the branching ratio is a strong function of $\alpha_2^{(0)}$. Table II gives the relative sizes of the ^{145}Tm ground-state wave function components and their associated decay widths, using a value of 0.084 for $\alpha_2^{(0)}$. As expected, the decay width to the 2^+ state is mainly due to the $l=3$ proton emission from the $7/2^- \otimes 2^+$ component of the wave function. Good agreement with the experimental spectroscopic factors is achieved, as shown in Table III. Since the $2f_{7/2}$ orbital lies in the next major shell, it should be virtually unoccupied and therefore its spectroscopic factor is unity. Experimental uncertainties in the proton energies and half-lives have been included in the uncertainties for the experimental spectroscopic factors S_{exp}. The theoretical spectroscopic factors S_{th} in column 7 have been taken from the low-seniority shell model calculation of Ref. [5], which assumes degeneracy of the $3s_{1/2}$, $2d_{3/2}$, and $1h_{11/2}$ shell model orbitals.

B. Other Odd-A Proton Emitters

The calculated decay widths and derived spectroscopic factors for other odd-A $68<Z<82$ proton emitters are shown in Table III. In cases where the EC/β^+ branches are unknown, they have been estimated using the calculated β-decay half-lives from Ref. [26], applying a 50% uncertainty. Fine structure has not been observed in any of these cases, mainly because the available proton energy for decay to the 2^+ state is much too small to allow an observable branch. Predicted branching ratios range from 10^{-4} to 10^{-16}.

Figure 3(a) shows the experimental spectroscopic factors S_{exp} for the odd-A proton emitters plotted as a function of p, the number of pairs of proton holes below $Z=82$ in the daughter nucleus. With the exception of ^{151}Lu^m and ^{177}Tl, they agree quite well with the low-seniority shell model calculation of spectroscopic factors described in Ref. [5], which is shown as a solid line in Fig. 3(a). For ^{177}Tl the $h_{11/2}$ and $s_{1/2}$ states are separated by 807 keV [24], and thus a spectroscopic factor calculated with the assumption of degenerate shell model orbitals will not be correct. The value of $S_{exp}=0.46(12)$ for ^{151}Lu^m obtained here can be compared with the value of $0.34(^{+12}_{-8})$ obtained using a purely spherical approach [19]. In contrast to previous work [3,5], the present value of S_{exp} for the other odd-A $d_{3/2}$ proton emitter ^{147}Tm^m agrees extremely well with the calculated value.

To demonstrate the importance of including particle-vibration coupling in the single-particle potential, Fig. 3(b) shows the experimental spectroscopic factors calculated in a

TABLE IV. Results of particle-vibrational coupling calculations for odd-odd spherical proton emitters with proton spin j_p. Experimental uncertainties in the proton energies and half-lives have been included in the uncertainties for the experimental spectroscopic factors S_{exp}. The calculated spectroscopic factors S_{th} are taken from Ref. [5].

Nuclide	j_p	$E_x(2^+)$ (keV)	$\alpha_2^{(0)}$	Γ(calc) (10^{-16} MeV)	Γ(exp) (10^{-16} MeV)	S_{exp}	S_{th}
^{146}Tm^m	$\frac{11}{2}^-$	326 [6]	0.084	5.81×10^{-5}	4.24×10^{-5} [27]	0.73(31)	0.78
^{146}Tm	$\frac{11}{2}^-$	326 [6]	0.084	8.84×10^{-6}	8.73×10^{-6} [27]	0.99(62)	0.78
^{150}Lu^m	$\frac{3}{2}^+$	600 [a]	0.059	0.437	0.152 [28]	$0.35(^{+36}_{-30})$	0.67
^{150}Lu	$\frac{11}{2}^-$	600 [a]	0.059	9.69×10^{-5}	6.33×10^{-5} [28]	0.65(18)	0.67
^{160}Re	$\frac{3}{2}^+$	800 [a]	0.049	1.65×10^{-2}	5.25×10^{-3} [29]	0.32(9)	0.44
^{164}Ir	$\frac{11}{2}^-$	660 [a]	0.052	0.139	7.86×10^{-2} [30]	0.57(29)	0.33
^{166}Ir^m	$\frac{11}{2}^-$	548 [22]	0.057	1.14×10^{-5}	4.98×10^{-6} [5]	0.44(18)	0.33
^{166}Ir	$\frac{3}{2}^+$	548 [22]	0.057	1.76×10^{-4}	3.00×10^{-5} [5]	0.17(9)	0.33
^{170}Au	$\frac{11}{2}^-$	582 [23]	0.054	1.82×10^{-2}	7.60×10^{-3} [30]	0.42(17)	0.22

[a]Estimated from energy systematics.

spherical picture for the same emitters as in Fig. 3(a). The agreement with the theoretical spectroscopic factors is now spoiled, clearly showing the important role played by particle-vibration coupling in the decay of near-spherical proton emitters.

C. Odd-Odd Proton Emitters

Table IV shows the results of decay width calculations for odd-odd proton emitters with $68<Z<82$. The extra neutron is treated as a spectator, and branches to excited states in the odd-A daughter, as have been observed in the decay of ^{146}Tm [6], are not included in the decay width. The experimental spectroscopic factors along with the low-seniority shell model calculation for the odd-odd proton emitters are shown in Fig. 3(c). The agreement is quite good, although the error bars are larger. Where the error bars are sufficiently small, it does appear that the S_{exp} values are still systematically lower than the calculations [3,5]. Further progress on these odd-odd cases requires higher precision energy and half-life measurements for existing and additional odd-odd proton emitters. Moreover, calculations including particle-vibration coupling between the unpaired neutron and the core should be performed.

IV. CONCLUSIONS

We have studied the influence of particle-vibration coupling on the decay rates of near-spherical proton emitters, in a coupled-channels formalism. The decay widths obtained are in good agreement with experiment, when spectroscopic factors from a low-seniority shell model calculation are used. The deviation between the calculated and experimental spectroscopic factors for emitters involving the $d_{3/2}$ proton orbital that was observed in previous work [3,5] has been eliminated or considerably reduced. We have here employed the same nuclear interaction between proton and core nucleus that was used in the successful description of the decay rates of the deformed proton emitters ^{131}Eu and ^{141}Ho [7].

In the case of odd-A proton emitters, the inclusion of particle-vibration coupling automatically yields the fine structure decay width to the first excited 2^+ state of the daughter nucleus, which cannot be obtained from one-dimensional spherical treatments. In ^{145}Tm [6], the one example where a measurement of fine structure in a near-spherical nucleus is available, excellent agreement with experiment is achieved with the use of particle-vibration coupling, for a ^{145}Tm ground-state spin of $J=11/2^-$. Assuming a permanent oblate deformation of $\beta_2=-0.18$ also produces agreement with experiment, but in this case the ground-state spin is $J=5/2^-$ and the state is not at the Fermi surface. Experiments to determine the ground-state spin of ^{145}Tm will be able to distinguish between these two alternatives.

For odd-odd proton emitters, good agreement with calculated spectroscopic factors was also achieved. In future, the situation will become clearer with the availability of higher precision experimental data on energies and half-lives, as well as additional examples of odd-odd emitters. Calculations including particle-vibration coupling of the unpaired neutron and pairing effects should also be investigated.

ACKNOWLEDGMENTS

The authors wish to acknowledge valuable discussions with R. Chasman and D. Kurath. This work was supported by the U.S. Department of Energy, Nuclear Physics Division, under Contract No. W-31-109-ENG-38.

[1] P.J. Woods and C.N. Davids, Annu. Rev. Nucl. Part. Sci. **47**, 541 (1997), and references therein.
[2] V.P. Bugrov *et al.*, Yad. Fiz. **41**, 1123 (1985) [Sov. J. Nucl. Phys. **41**, 717 (1985)].
[3] S. Åberg, P.B. Semmes, and W. Nazarewicz, Phys. Rev. C **56**, 1762 (1997); **58**, 3011 (1998).
[4] E. Maglione, L.S. Ferreira, and R.J. Liotta, Phys. Rev. Lett. **81**, 538 (1998).
[5] C.N. Davids *et al.*, Phys. Rev. C **55**, 2255 (1997).
[6] K.P. Rykaczewski *et al.*, Nucl. Phys. **A682**, 270c (2001); J. C. Batchelder (private communication).
[7] H. Esbensen and C.N. Davids, Phys. Rev. C **63**, 014315 (2001).
[8] L.S. Ferreira and E. Maglione, Phys. Rev. C **61**, 021304(R) (2000).
[9] P. Möller *et al.*, At. Data Nucl. Data Tables **59**, 185 (1995).
[10] Y. Aboussir *et al.*, At. Data Nucl. Data Tables **61**, 127 (1995).
[11] G. Lalazissis, D. Vretenar, and P. Ring, Nucl. Phys. **A650**, 133 (1999).
[12] P.B. Semmes, Nucl. Phys. **A682**, 239c (2001).
[13] A. Bohr and B. R. Mottelson, *Nuclear Structure* (Benjamin, Reading, MA, 1975), Vol. II.
[14] S. Raman *et al.*, Phys. Rev. C **43**, 556 (1991), Eq. (4).
[15] C.N. Davids and H. Esbensen, Phys. Rev. C **61**, 054302 (2000).
[16] J.H. McNeill *et al.*, Z. Phys. A **344**, 369 (1993).
[17] D. Seweryniak, Proceedings of the Conference on Nuclear Structure at the Limits, 1996, Argonne National Laboratory Report No. ANL/PHY-97/1, 1997, p. 247.
[18] P. Sellin *et al.*, Phys. Rev. C **47**, 1933 (1993).
[19] C.R. Bingham *et al.*, Phys. Rev. C **59**, R2984 (1999).
[20] A. Keenan *et al.*, Phys. Rev. C **63**, 064309 (2001).
[21] R.J. Irvine *et al.*, Phys. Rev. C **55**, R1621 (1997).
[22] S.L. King *et al.*, Phys. Rev. C **62**, 067301 (2000).
[23] S.L. King *et al.*, Phys. Lett. B **443**, 82 (1998).
[24] G.L. Poli *et al.*, Phys. Rev. C **59**, R2979 (1999).
[25] M.P. Carpenter *et al.*, Phys. Rev. Lett. **78**, 3650 (1997).
[26] P. Möller, J.R. Nix, and K.-L. Kratz, At. Data Nucl. Data Tables **66**, 131 (1997).
[27] K. Livingston *et al.*, Phys. Lett. B **312**, 46 (1993).
[28] T.N. Ginter *et al.*, Phys. Rev. C **61**, 014308 (1999).
[29] R.D. Page *et al.*, Phys. Rev. Lett. **68**, 1287 (1992).
[30] H. Mahmud (private communication).